

# Zero-Shot Reconstruction of Animatable 3D Avatars with Cloth Dynamics from a Single Image

Joohyun Kwon    Geonhee Sim    Gyeongsik Moon  
Korea University

{juheanqueen, kh6362, mks0601}@korea.ac.kr

<https://juhyeon-kwon.github.io/DynaAvatar.github.io/>

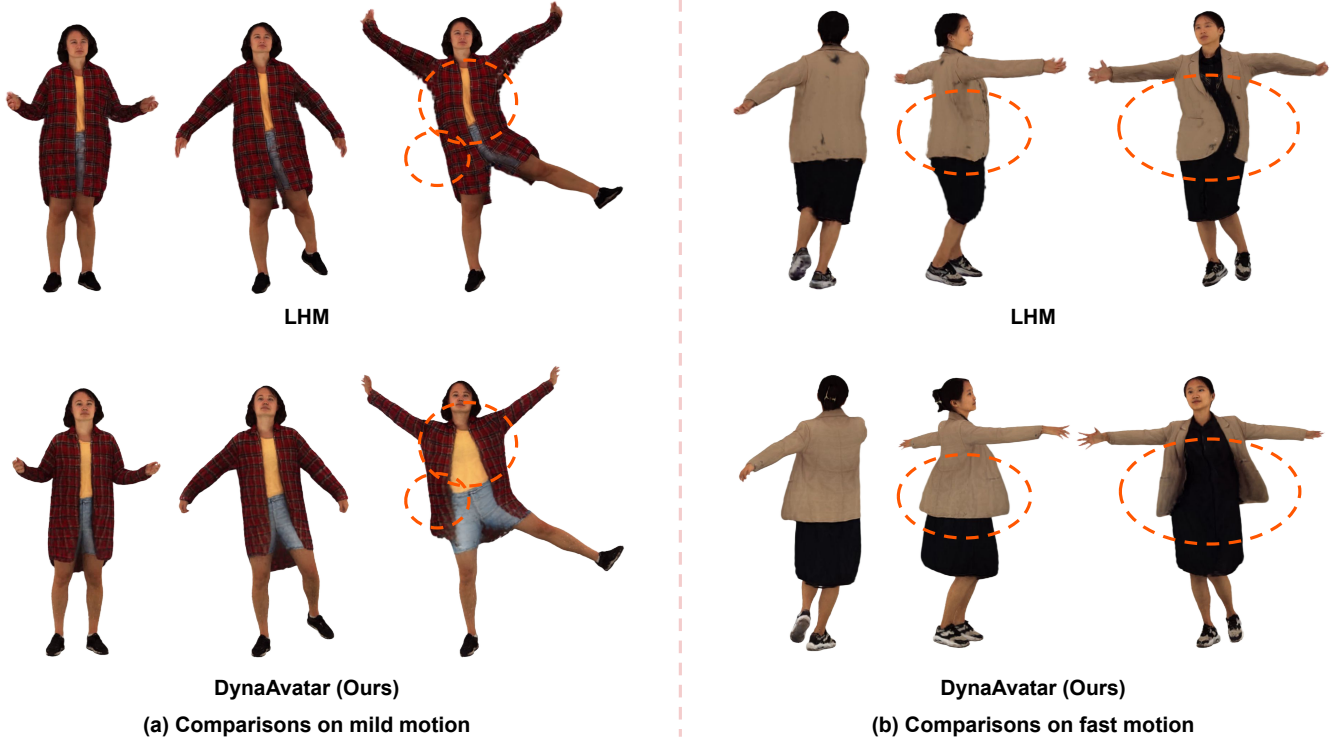


Figure 1. Comparison between LHM [38] and our DynaAvatar on both mild and fast motions. Unlike prior single-image-based methods, DynaAvatar can reconstruct animatable 3D human avatars that exhibit motion-dependent cloth dynamics.

## Abstract

Existing single-image 3D human avatar methods primarily rely on rigid joint transformations, limiting their ability to model realistic cloth dynamics. We present **DynaAvatar**, a zero-shot framework that reconstructs animatable 3D human avatars with motion-dependent cloth dynamics from a single image. Trained on large-scale multi-person motion datasets, DynaAvatar employs a Transformer-based feed-forward architecture that directly predicts dynamic 3D Gaussian deformations without subject-specific optimization. To overcome the scarcity of dynamic captures, we introduce a static-to-dynamic knowledge transfer strategy: a Transformer pretrained on large-scale static cap-

tures provides strong geometric and appearance priors, which are efficiently adapted to motion-dependent deformations through lightweight LoRA fine-tuning on dynamic captures. We further propose the DynaFlow loss, an optical flow-guided objective that provides reliable motion-direction geometric cues for cloth dynamics in rendered space. Finally, we reannotate the missing or noisy SMPL-X fittings in existing dynamic capture datasets, as most public dynamic capture datasets contain incomplete or unreliable fittings that are unsuitable for training high-quality 3D avatar reconstruction models. Experiments demonstrate that DynaAvatar produces visually rich and generalizable animations, outperforming prior methods.

# 1. Introduction

Creating realistic and animatable 3D human avatars from monocular inputs has long been a fundamental goal in computer vision, graphics, and virtual human research. Most existing single-image animatable avatar reconstruction methods [38, 40, 61] are limited to skeletal-based deformation, where the human body is animated primarily by rigid transformations of body joints. While effective for body articulation, such representations inherently lack the ability to model non-rigid cloth dynamics, resulting in over-rigid motion and a loss of visual realism during animation.

Several personalized avatar methods [1, 22, 24, 31, 35, 36, 50, 58] reconstruct dynamic human models from multi-view videos of individual subjects. Although these approaches capture subject-specific geometry and clothing deformation, they require a separate capture and optimization process for each person, making them impractical to apply to arbitrary subjects. This dependency on multi-view capture severely limits their scalability and usability, especially when animatable avatars are needed for new individuals without dedicated data collection.

In this work, we present **DynaAvatar**, a novel framework that generates animatable 3D avatars with motion-dependent cloth dynamics from a single image in a zero-shot manner. We define zero-shot as the ability to reconstruct avatars for unseen identities without any subject-specific fine-tuning or optimization. Unlike personalized approaches [1, 22, 24, 30, 31, 35, 36, 40, 44, 50, 58], which fit a model to each individual, DynaAvatar learns motion-dependent deformation priors that generalize across identities, enabling feed-forward avatar reconstruction. Our Transformer [7, 47]-based feed-forward architecture directly predicts dynamic 3D Gaussian deformations without any subject-specific optimization, allowing fast and scalable avatar reconstruction.

To address the limited availability of large-scale dynamic captures covering diverse clothing and motions, we introduce a static-to-dynamic knowledge transfer strategy that leverages pretrained static representations for dynamic learning. We adopt a Transformer pretrained on large-scale static captures to provide strong geometric and appearance priors of human bodies and garments. During dynamic training, we incorporate a Dynamic Transformer trained from scratch to specialize in motion-dependent deformation modeling, while efficiently adapting the pretrained Static Transformer using lightweight LoRA adapters [15]. This transfer-based design enables DynaAvatar to inherit rich static knowledge for geometry and appearance, while effectively learning motion-aware dynamic behaviors even with limited dynamic supervision.

To further enhance the learning of large and complex cloth movements, we introduce the DynaFlow loss function, an optical flow-guided correspondence loss that pro-

Table 1. Comparison of existing avatar reconstruction methods and the proposed DynaAvatar. Each column indicates whether the method reconstructs avatars in a zero-shot manner (*i.e.*, without subject-specific optimization), whether it supports cloth dynamics, and whether it operates from a single input image.

Methods	Zero shot	Cloth dynamics	Single image
ExAvatar [30]	✗	✗	✗
IDOL [61]	✓	✗	✓
AniGS [40]	✗	✗	✓
LHM [38]	✓	✗	✓
PERSONA [44]	✗	✓	✓
MPMAvatar [23]	✗	✓	✗
SeqAvatar [50]	✗	✓	✗
<b>DynaAvatar (Ours)</b>	✓	✓	✓

vides explicit pixel-wise motion-direction cues in the rendered screen space. Unlike conventional image-space reconstruction losses that rely on local pixel similarity, DynaFlow leverages optical flow to establish reliable correspondences even under fast or large non-rigid cloth deformations, while providing geometry-only supervision that avoids the color-geometry ambiguity inherent to image losses. This leads to a more accurate modeling of motion-dependent cloth dynamics.

Finally, we reannotate existing dynamic capture datasets [5, 19, 48] with accurate SMPL-X [34] fittings. Although existing dynamic capture datasets provide multi-view videos with diverse clothing and motions, they often include missing or highly noisy SMPL-X parameters, making them unsuitable for training high-quality 3D avatar reconstruction models. Our reannotation yields accurate and complete SMPL-X parameters, enabling over 11M high-quality image supervisions.

By integrating the static-to-dynamic knowledge transfer, DynaFlow loss function, and reannotated fittings, DynaAvatar effectively captures realistic and temporally coherent cloth dynamics across diverse motions. Extensive experiments confirm that our framework significantly improves the realism and generalization of single-image 3D avatar generation, bridging the gap between static reconstruction and dynamic animation.

Our main contributions are as follows:

- We propose DynaAvatar, the first zero-shot framework that reconstructs animatable 3D avatars with motion-dependent cloth dynamics from a single image.
- We introduce a static-to-dynamic knowledge transfer strategy that leverages pretrained static representations for geometry and appearance, and fine-tunes them with lightweight LoRA adaptation to learn motion-dependent deformations.
- We propose the DynaFlow loss function, an optical flow-guided correspondence loss that provides pixel-wise motion-direction cues for more accurate supervision of large and complex cloth dynamics, offering geometry-only guidance that avoids the color-geometry ambiguity

of image losses.

- We reannotate existing dynamic capture datasets to curate a refined dataset with accurate SMPL-X parameters, providing consistent and reliable supervision for dynamic avatar training.

## 2. Related works

### Zero-shot 3D animatable avatars from a single image.

Zero-shot 3D animatable avatar reconstruction methods aim to reconstruct avatars in a feed-forward manner without any subject-specific optimization, by being trained on large-scale datasets. Since they eliminate the need for per-subject optimization, they achieve significantly shorter inference times compared to methods that rely on personalized fitting. IDOL [61] is trained on a large-scale generated dataset to reconstruct 3D Gaussian avatars from a single image. LHM [38] follows the spirit of IDOL by adopting a multimodal Transformer [7, 47] architecture for zero-shot 3D human reconstruction, while PF-LHM [39] further explores pose-free multi-image inputs for improved reconstruction robustness. However, all of the above methods have limited animation fidelity, as they primarily rely on rigid body joint transformations for animation. In contrast, our DynaAvatar is a zero-shot framework that can effectively model motion-dependent cloth dynamics, enabling more realistic and expressive avatar animations.

**3D animatable avatars with subject-specific optimizations.** Peng *et al.* [35, 36] and Zheng *et al.* [58] optimize personalized NeRF [29]-based avatars using multi-view videos of each individual. GaussianAvatar [16] and ExAvatar [30] instead optimize personalized 3DGS [20]-based avatars from monocular videos. Dyco [4] introduce delta pose sequence to effectively model temporal appearance variations. AniGS [40] synthesizes multi-view images and optimizes a 3DGS-based avatar on them, while PERSONA [44] generates pose-rich videos for optimization. SeqAvatar [50], MPMAvatar [23], and Zhan *et al.* [55] perform optimization on multi-view videos. All of the above methods rely on subject-specific optimization, making them unsuitable for arbitrary individuals when video captures are unavailable. Although some methods [40, 44] support single-image optimization, they still suffer from slow inference compared to feed-forward architectures.

**Cloth dynamics.** Early works [10, 12, 37] focused on 3D clothing reconstruction without animation capability. More recent studies aim to recover simulation-ready 3D garment representations, where physics-based simulation is used to animate the reconstructed garments. HOOD [8] leverages graph neural networks, multi-level message passing, and unsupervised training to predict realistic clothing dynamics, while ContourCraft [9], built upon HOOD, further resolves garment interpenetrations. GaussianGarment [42] represents clothing using a hybrid of 3D meshes and Gaussian

textures, and PGC [11] reconstructs simulation-ready garments from multi-view images of a static human pose. AIpparel [32] and ChatGarment [2] enable single-image garment recovery by predicting simulation-ready clothing representations such as sewing patterns or parametric meshes.

Despite their progress, these physics-driven or simulation-based approaches face several limitations. They either require clean cloth meshes or calibrated multi-view captures, which are difficult to obtain in real-world settings, or rely on automatically estimated 3D poses that are often inaccurate for in-the-wild single images or monocular videos. Such imperfect or penetrating poses frequently cause instability in physics-based systems, resulting in cloth drifting and physically implausible deformations. In contrast, our DynaAvatar learns data-driven, motion-dependent deformations without relying on explicit physical constraints, maintaining stability even under imperfect pose conditions. Moreover, our framework reconstructs a full-body photorealistic avatar, whereas prior methods focus solely on clothing geometry without modeling the entire human body.

**Generative human animation.** With the rapid progress of image and video generative models [3, 14], many approaches animate a person from a single reference image using 2D pose sequences. These methods directly generate human videos without explicit 3D representations. Diffusion-based frameworks [17, 51, 57] improve temporal coherence and pose control, while others [28, 46] enhance spatial consistency and identity preservation. SMPL-conditioned models [18, 43, 60] enable controllable motion, and additional works extend facial motion or implicit motion modeling [27, 45]. Although these models produce photorealistic results, they remain tied to their training setup: inputs and poses must be pixel-aligned, subjects must stay near the image center, and outputs have fixed resolution. In contrast, DynaAvatar builds upon 3DGS [20], supporting arbitrary poses, spatial layouts, and scalable resolutions with consistent 3D geometry and appearance.

## 3. DynaAvatar

### 3.1. Pipeline

Fig. 2 illustrates the overall pipeline of the proposed DynaAvatar. Given a single image of an arbitrary person, DynaAvatar extracts features using two Transformer modules [7, 47].

**Static Transformer.** The Static Transformer captures detailed geometry and appearance without modeling cloth dynamics. It takes image tokens  $\mathbf{T}_I$  extracted from the input image via pretrained encoders (Sapiens [21] and DINOv2 [33]) as keys and values, while initial 3D point tokens  $\mathbf{T}_{3D}$  (*i.e.*, positional encoding [29] of SMPL-X template vertices), serve as queries. We freeze the pre-trained

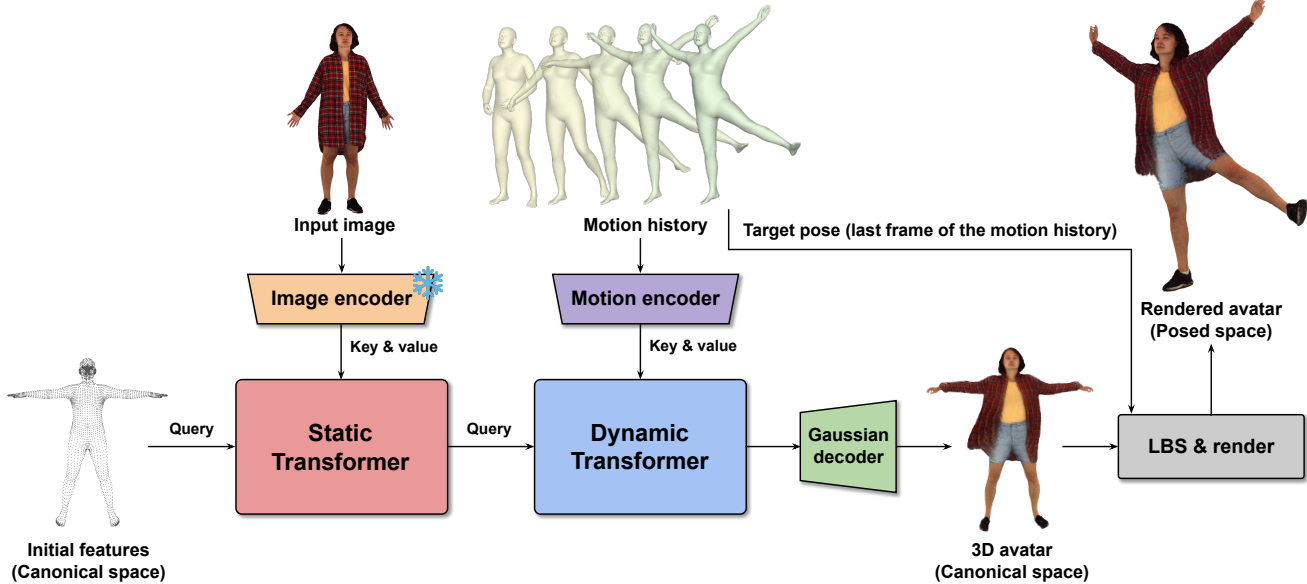


Figure 2. Overall pipeline of the proposed DynaAvatar. We first extract detailed geometry and appearance without cloth dynamics using a Static Transformer. Next, cloth dynamics are incorporated from motion history through a Dynamic Transformer. The final 3D avatar in canonical space is reconstructed using a Gaussian decoder and then animated and rendered with LBS and a 3DGS renderer. Since the canonical avatar already encodes motion-dependent cloth dynamics, the animation produced by LBS faithfully maintains these dynamics.

image encoder. The 3D point tokens are then updated using a Multimodal Transformer Block (MM) [7]:  $\mathbf{T}_{3D}, \mathbf{T}_I \leftarrow \text{MM}(\mathbf{T}_{3D}, \mathbf{T}_I; \mathbf{F}_I)$ . The global context feature  $\mathbf{F}_I$ , obtained by averaging Sapiens image tokens, is used for modulation via Adaptive Layer Normalization (AdaLN).

**Motion encoder.** A motion encoder processes the motion history covering one second (15 time steps) to produce a motion tokens  $\mathbf{T}_M$ . The motion history includes 3D poses, 3D pose velocities, 3D pose accelerations, and 3D key-point velocities, where each pose is represented using the 6D rotation parameterization [59]. If the motion history is unavailable (*e.g.*, the first frame of a video or a single-image demonstration), all past motions—excluding the current frame—are initialized to zero. To ensure consistency, the motion history is transformed into a canonical world coordinate system, as the up-vector of each 3D pose may vary. When world axes are provided by the dataset, they are used for alignment; otherwise, the camera’s  $y$ -axis is assumed as the up-vector. This normalization prevents inconsistencies in motion semantics across poses. The motion encoder consists of positional encoding followed by several multi-layer perceptrons (MLPs).

**Dynamic Transformer.** The Dynamic Transformer refines the static features by integrating motion-aware cloth dynamics. The motion tokens  $\mathbf{T}_M$  produced by the motion encoder, together with the Static Transformer output  $\mathbf{T}_{3D}$ , are fed into the Dynamic Transformer. Specifically,  $\mathbf{T}_M$  acts as keys and values, while  $\mathbf{T}_{3D}$  serves as queries within its MM [7]:  $\mathbf{T}_{3D}, \mathbf{T}_M \leftarrow \text{MM}(\mathbf{T}_{3D}, \mathbf{T}_M; \mathbf{F}_M)$ . The pose fea-

ture  $\mathbf{F}_M$  is defined as the last element of  $\mathbf{T}_M$  and serves as the condition for AdaLN.

**Gaussian Decoder.** The output features from the Dynamic Transformer are fed into a Gaussian decoder, which reconstructs 3DGS [20] representations (*i.e.*, mean, scale, rotation, opacity, and color) to form the final avatar in the canonical space with motion-dependent cloth dynamics. In addition, it predicts skinning weight offsets, enabling each Gaussian to adapt its animation based on the motion history. The decoder itself is implemented as a single linear layer.

**Animation and Rendering.** Finally, the canonical avatar is animated using LBS with refined skinning weights, which combine the predicted offsets with diffused skinning weights [37, 44], and rendered using a 3DGS renderer. Note that the canonical avatar already encodes motion-dependent cloth dynamics, while the refined skinning weights further enhance these dynamics; thus, applying LBS naturally preserves realistic motion during animation.

### 3.2. Static-to-dynamic knowledge transfer

Learning realistic motion-dependent cloth dynamics ideally requires large-scale dynamic capture datasets, which are extremely costly to collect due to multi-view synchronization, temporal calibration, and garment diversity requirements [5, 19, 48, 49]. In contrast, static captures [13, 26, 41, 54, 61] are far more abundant and provide high-quality geometry and appearance supervision, though they lack temporal deformation cues.

Following the recent paradigm of leveraging large pre-trained models for knowledge transfer [17, 28, 46, 51,

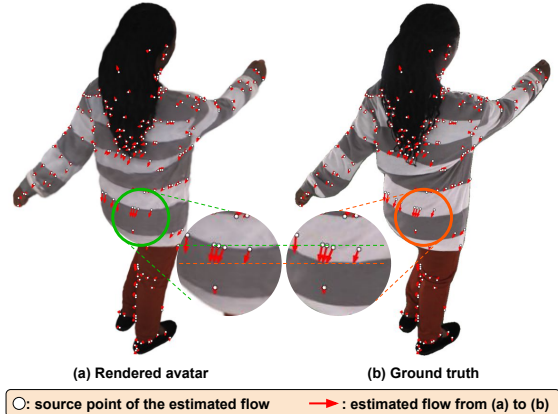


Figure 3. Visualization of the proposed DynaFlow loss. Our DynaFlow loss encourages the Gaussians at source locations (black-outlined white circles) to move toward the endpoints of the estimated flow vectors.

[57], we adopt a Transformer pretrained on large-scale static captures [38] as the static backbone of DynaAvatar. This pretrained model provides strong geometric and appearance priors that facilitate the subsequent learning of motion-dependent dynamics. During dynamic training, we introduce a Dynamic Transformer trained from scratch while fine-tuning the pretrained Static Transformer using lightweight LoRA adapters [15]. This transfer-based adaptation allows DynaAvatar to effectively learn realistic cloth dynamics even with limited dynamic supervision, benefiting from knowledge distilled from large-scale static data.

### 3.3. DynaFlow loss function

Image reconstruction losses entangle geometry and color, creating ambiguity that weakens geometric supervision. They also operate on local patches, making them ineffective for strong cloth deformations that require long-range correspondence. To address these limitations, we introduce DynaFlow loss function  $\mathcal{L}_{\text{flow}}$ , a geometry-only, flow-based supervision that provides explicit, deformation-aligned correspondence cues. By decoupling geometry from appearance, DynaFlow supplies structural signals that image losses cannot capture, enabling accurate modeling of large and complex cloth motions. Fig. 3 illustrates our DynaFlow loss, which leverages optical flow to establish correspondences between the rendered and ground-truth images even when deformation exceeds the receptive field of conventional losses.

To extract robust geometric cues, we render not only an RGB image but also an  $xy$  map  $\mathbf{M} \in \mathbb{R}^{H \times W \times 2}$  substituting Gaussian colors with their projected screen-space  $xy$  coordinates. We compute optical flow between the rendered and ground truth images using LightGlue [25], obtaining  $N$  matched source and target pixel coordinates,  $\mathbf{p}_{\text{src}}$  and  $\mathbf{p}_{\text{tgt}}$ , respectively. By grid-sampling the  $xy$  map  $\mathbf{M}$  at  $\mathbf{p}_{\text{src}}$  and

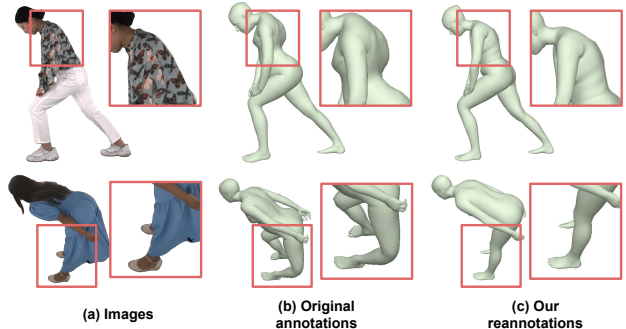


Figure 4. Comparison between (b) the original annotations and (c) our reannotations for the DNA-Rendering [5] (top) and Actors-HQ [19] (bottom) datasets.

enforcing the sampled coordinates to match the flow targets  $\mathbf{p}_{\text{tgt}}$ , DynaFlow injects direct pixel-level displacement supervision, defined as:  $\mathcal{L}_{\text{flow}} = \frac{1}{N} \sum \|\mathbf{M}(\mathbf{p}_{\text{src}}) - \mathbf{p}_{\text{tgt}}\|_1$ . This design allows gradients to backpropagate through  $\mathbf{M}$ , thereby directly correcting the 2D positions of the Gaussians. Our DynaFlow loss resolves the geometry–color entanglement that causes image losses to blur or smooth out large cloth motions, allowing our model to reconstruct sharper boundaries and more faithful dynamic deformations. We cap the number of matches  $N$  at 1024 for stability, and LightGlue’s efficiency keeps the additional training cost minimal. The  $\mathcal{L}_{\text{flow}}$  is activated only after the midpoint of training, since early-stage renderings are inaccurate and produce unreliable optical flow.

In addition to DynaFlow, we supervise the rendered avatars using a combination of  $L1$ , SSIM, mask, and LPIPS [56] losses. We further adopt geometry regularizers from prior works [30, 44], including the Laplacian regularizer, to stabilize face and hand geometry—regions that occupy only a small portion of the image and thus receive weak direct supervision.

## 4. Reannotating dynamic capture datasets

Fig. 4 compares (b) existing SMPL-X fittings and (c) our reannotated results. Our reannotation yields accurate and complete SMPL-X parameters, enabling over 11M high-quality image supervisions. Although multiple dynamic capture datasets have been introduced [5, 19, 48, 49], most are not directly suitable for training or evaluating DynaAvatar due to incomplete or noisy SMPL-X annotations. DNA-Rendering [5] provides SMPL-X fittings for only about 20% of frames, and even those often exhibit significant errors and temporal jitter. MVHumanNet [49] offers downsampled sequences at only 5 frames per second, which is insufficient for modeling motion-dependent cloth dynamics. 4D-Dress [48] provides only gender-specific fittings without gender-neutral counterparts, while most 3D avatar reconstruction methods [38, 61] (including ours) require

gender-neutral models for consistency. Actors-HQ [19] also contains inaccurate SMPL-X fittings. Such inaccuracies lead to pixel misalignment between the rendered outputs and the target images, severely degrading supervision quality, as the primary image reconstruction loss assumes approximate pixel alignment between the rendered avatar and the ground-truth image.

To address the missing or noisy original annotations, we reconstruct refined SMPL-X fittings for all frames using a unified reannotation pipeline. We first predict 2D whole-body keypoints for all images using DWPose [52] and initialize SMPL-X parameters from the frontal-view image via SMLest-X [53]. The 3D translation is triangulated from 2D keypoints with confidence above 0.3, and SMPL-X parameters are optimized by minimizing the  $L_1$  distance between projected and predicted 2D keypoints across all views with confidence above 0.3. Additional regularization terms suppress unnatural head leaning and foot bending, and the results are temporally smoothed using a Savitzky–Golay filter for stability. While existing fittings rely on triangulated 3D keypoints that are prone to triangulation errors, our pipeline directly leverages multi-view 2D keypoints, eliminating such errors and achieving higher fitting accuracy.

We manually inspected all fittings by rendering them as multi-view videos, checking both pixel-level alignment and temporal consistency. Captures with unreliable 2D keypoints—typically from subjects wearing extremely loose clothing—are excluded from training. In such cases, the underlying body pose is heavily occluded by the cloth, making keypoint detection difficult and resulting in noisy original SMPL-X fittings. We also exclude captures involving human–object interactions, which are manually identified, since objects are not part of our avatar modeling. Finally, we omit the mask loss during optimization because the SMPL-X model represents only the naked body, and using mask supervision led to body-shape distortions for subjects wearing loose garments.

## 5. Experiments

### 5.1. Datasets and evaluation metrics

**Datasets.** DNA-Rendering [5] and 4D-Dress [48] are used for training, and we evaluate on DNA-Rendering, 4D-Dress, and Actors-HQ [19]. For DNA-Rendering, we split the dataset so that training and testing subjects do not overlap. For 4D-Dress, we render each 3D scan from 24 uniformly placed virtual cameras, ensuring that the test set contains novel subjects and clothing. We use all 14 sequences of Actors-HQ with the 39 visible cameras. Actors-HQ is not used for training and therefore serves as a cross-domain generalization benchmark. These datasets provide high-resolution videos of diverse subjects, motions, and cloth dynamics, making them well suited for assessing dynamic

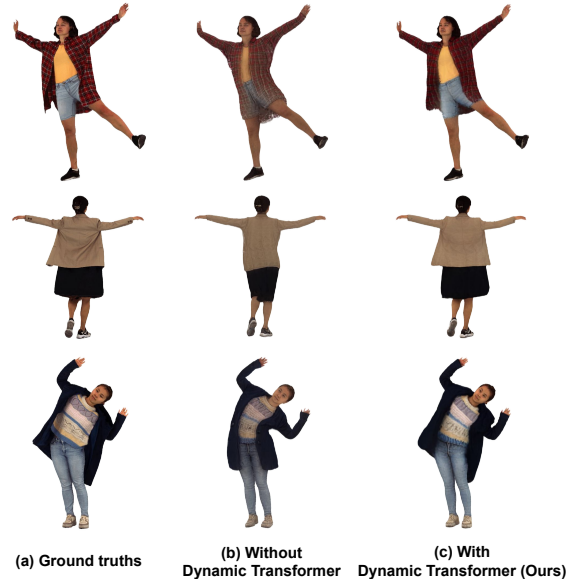


Figure 5. Effectiveness of our Dynamic Transformer.

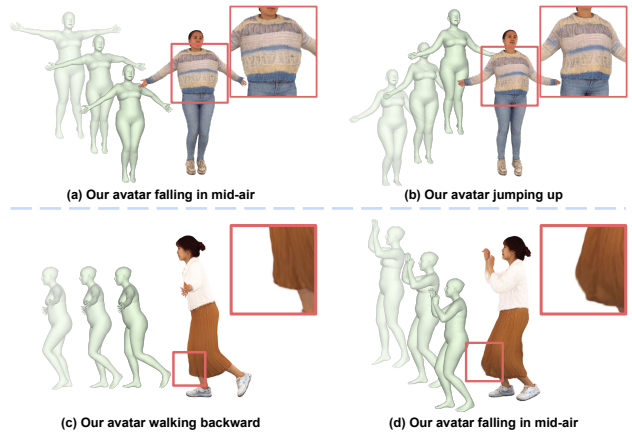


Figure 6. Rendered avatars in similar poses but different motion histories. (a) and (b) share similar poses, but (a) is falling in mid-air while (b) is jumping up. (c) and (d) also exhibit similar poses, with (c) walking backward and (d) falling in mid-air. Despite having nearly identical poses, their clothing appears clearly different because our Dynamic Transformer effectively handles different motion information.

Table 2. Effectiveness of our Dynamic Transformer on 4D-Dress.

Settings	PSNR $\uparrow$	SSIM $\uparrow$	LPIPS $\downarrow$
Wo. Dynamic Transformer	22.57	0.952	0.068
<b>DynaAvatar (Ours)</b>	<b>23.62</b>	<b>0.958</b>	<b>0.062</b>

avatar reconstruction. As described in Sec. 4, we use our reannotated SMPL-X fittings for all experiments including baselines and previous works.

**Evaluation metrics.** Following previous works [30, 38, 40, 44, 50, 61], we use PSNR, SSIM, and LPIPS [56] as evaluation metrics, which measure the similarity between the rendered and the ground truth images.

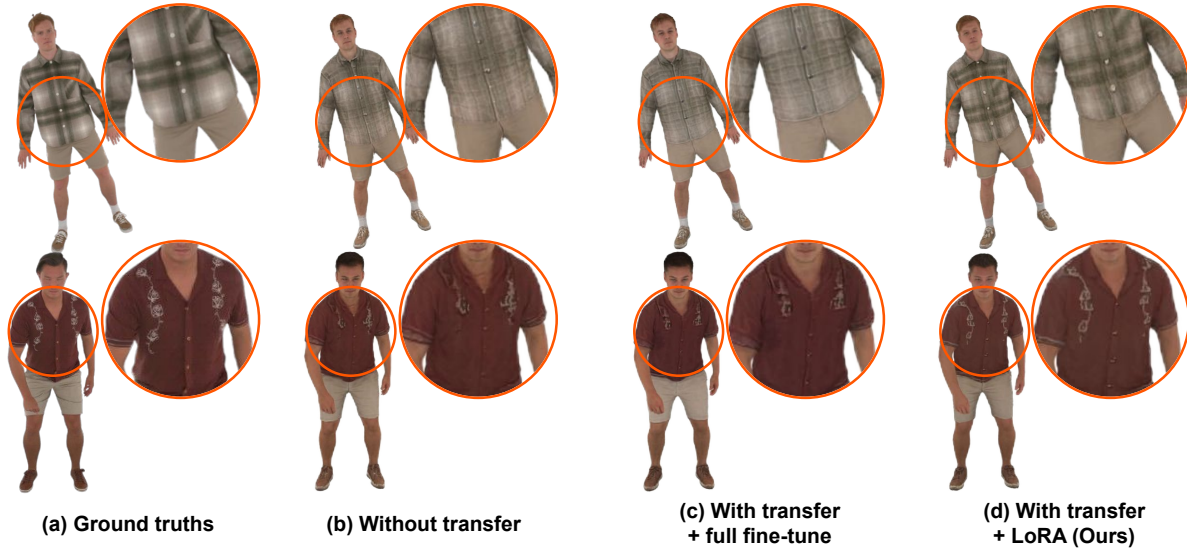


Figure 7. Effectiveness of our static-to-dynamic knowledge transfer with LoRA.



Figure 8. Effectiveness of our DynaFlow loss function.

## 5.2. Ablation studies

**Dynamic Transformer.** Fig. 5 and Tab. 2 show that our Dynamic Transformer is essential for modeling motion-dependent cloth dynamics. Fig. 6 shows that our avatars exhibit clearly different cloth deformations even though they share similar poses and originate from the same input images. Since the only difference between the two cases is the motion history, this result demonstrates that our Dynamic Transformer effectively provides essential motion information. A baseline without the Dynamic Transformer instead uses a Static Transformer with LoRA [15] to extract Gaussian features, which are then fed into the Gaussian decoder. However, because this baseline does not incorporate motion history—similar to prior single-image methods [38, 40, 61]—its ability to represent dynamic deformations is fundamentally limited.

**Static-to-dynamic knowledge transfer.** Fig. 7 shows that our static-to-dynamic knowledge transfer with LoRA achieves the best results. To validate this design, we evaluate two baselines. First ((b)), we randomly initialize the Static Transformer and train it from scratch, introducing no knowledge transfer from pretrained static models. Second ((c)), we fully fine-tune the pretrained Static Transformer without LoRA. As shown in the figure, both (b) and (c) fail to preserve the texture patterns of the person in the input image. This analysis demonstrates that knowledge transfer from static captures is beneficial, and that LoRA is essential for preserving this knowledge while enabling the Dynamic Transformer to learn motion-dependent cloth dynamics.

**DynaFlow loss function.** Fig. 8 shows that our DynaFlow loss function is highly effective in modeling both large cloth motions and clear cloth boundaries. The two examples

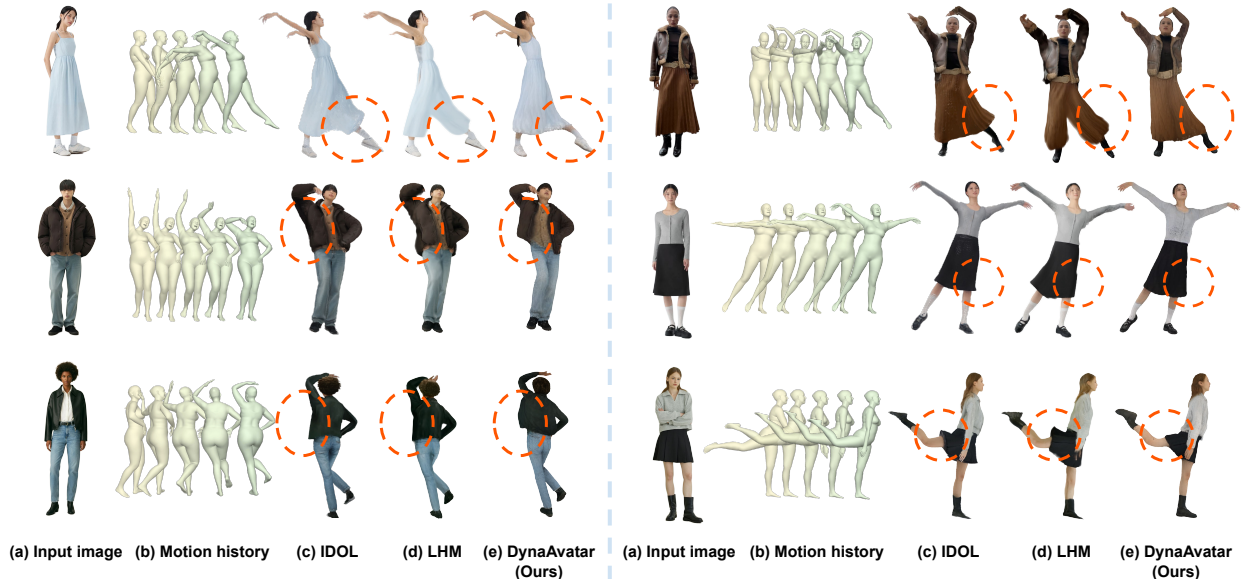


Figure 9. Comparison between DynaAvatar and previous single-image-based state-of-the-art methods [38, 61] on in-the-wild images.

Table 3. Comparison between DynaAvatar and previous single-image-based state-of-the-art methods.

Methods	DNA-Rendering [5]			4D-Dress [48]			Actors-HQ [19]		
	PSNR $\uparrow$	SSIM $\uparrow$	LPIPS $\downarrow$	PSNR $\uparrow$	SSIM $\uparrow$	LPIPS $\downarrow$	PSNR $\uparrow$	SSIM $\uparrow$	LPIPS $\downarrow$
IDOL [61]	17.84	0.902	0.155	21.31	0.948	0.077	20.93	0.910	0.138
PERSONA [44]	14.91	0.883	0.207	19.46	0.943	0.098	19.08	0.904	0.171
LHM [38]	17.42	0.901	0.169	21.03	0.950	0.085	20.29	0.908	0.151
<b>DynaAvatar (Ours)</b>	<b>19.45</b>	<b>0.916</b>	<b>0.136</b>	<b>23.74</b>	<b>0.960</b>	<b>0.064</b>	<b>21.38</b>	<b>0.916</b>	<b>0.128</b>

in the left column demonstrate that DynaFlow enables the model to recover large, sweeping cloth dynamics. Without DynaFlow, the model relies solely on image reconstruction losses, which operate on local patches and therefore struggle to establish accurate correspondences under large deformations—resulting in clothes that remain nearly static. The two examples in the right column show that DynaFlow also produces noticeably cleaner cloth boundaries; in contrast, without it, the boundaries often collapse or blend into neighboring regions. This improvement stems from the geometry-only, flow-based supervision provided by DynaFlow, which removes the color-geometry ambiguity inherent to image losses. By injecting explicit pixel-displacement cues that tell each Gaussian how it should move, DynaFlow allows the model to recover both large-scale deformations and sharp, well-separated boundary details that standard image losses alone cannot supervise.

### 5.3. Comparisons to state-of-the-art methods

Fig. 9 and Tab. 3 show that DynaAvatar outperforms prior single-image 3D animatable avatar methods [38, 44, 61]. Qualitatively, DynaAvatar models motion-dependent cloth dynamics far more faithfully, even for in-the-wild examples.

In contrast, IDOL [61] and LHM [38] largely preserve the cloth deformation from the input image rather than adapting it to motion. As seen in the left-top example, the

skirt is copied directly, causing unnatural ankle overlap; in the left-middle and left-bottom cases, the jacket fails to lift during upward motion; and in the right column, the skirt remains static across poses.

DynaAvatar succeeds because the Dynamic Transformer incorporates motion cues and is trained with the DynaFlow loss, which provides geometry-only, flow-based correspondence signals that resolve the color-geometry ambiguity of conventional image losses. All previous methods are evaluated using their official implementations with our reannotated SMPL-X fittings. For LHM, we compare against the 500M model to match our Static Transformer’s scale, and PF-LHM is excluded due to the lack of publicly available code.

## 6. Conclusion

We presented DynaAvatar, a zero-shot framework that reconstructs animatable 3D avatars with motion-dependent cloth dynamics from a single image. Through static-to-dynamic knowledge transfer and the proposed DynaFlow loss, our method effectively learns dynamic deformations. Our reannotated fittings further provide reliable supervision for training dynamic avatars. We believe DynaAvatar offers a promising step toward more expressive single-image avatar generation.

## Acknowledgments

This work was partly supported by the Institute of Information & Communications Technology Planning & Evaluation(IITP)-ICT Creative Consilience Program grant funded by the Korea government(MSIT)(IITP-2026-RS-2020-II201819, 20%). This research was supported by the Culture, Sports and Tourism R&D Program through the Korea Creative Content Agency grant funded by the Ministry of Culture, Sports and Tourism in 2026(Project Name: Development of AI-based image expansion and service technology for high-resolution (8K/16K) service of performance contents, Project Number: RS-2024-00395886, Contribution Rate: 20%). This work was supported by the Industrial Technology Innovation Program(RS-2025-02653087, Development of a Motion Data Collection System and Dynamic Persona Modeling Technology) funded By the Ministry of Trade, Industry & Energy(MOTIE, Korea). This work was supported by the IITP grant funded by the MSIT (No. RS-2025-25441838, Development of a human foundation model for human-centric universal artificial intelligence and training of personnel). This work was supported by the National Research Foundation of Korea(NRF) grant funded by the Korea government(MSIT)(RS-2025-21063115).

## References

- [1] Timur Bagautdinov, Chenglei Wu, Tomas Simon, Fabian Prada, Takaaki Shiratori, Shih-En Wei, Weipeng Xu, Yaser Sheikh, and Jason Saragih. Driving-signal aware full-body avatars. *ACM TOG*, 2021. 2
- [2] Siyuan Bian, Chenghao Xu, Yuliang Xiu, Artur Grigorev, Zhen Liu, Cewu Lu, Michael J Black, and Yao Feng. ChatGarment: Garment estimation, generation and editing via large language models. In *CVPR*, 2025. 3
- [3] Andreas Blattmann, Tim Dockhorn, Sumith Kulal, Daniel Mendelevitch, Maciej Kilian, Dominik Lorenz, Yam Levi, Zion English, Vikram Voleti, Adam Letts, et al. Stable Video Diffusion: Scaling latent video diffusion models to large datasets. *arXiv preprint arXiv:2311.15127*, 2023. 3
- [4] Yutong Chen, Yifan Zhan, Zhihang Zhong, Wei Wang, Xiao Sun, Yu Qiao, and Yinqiang Zheng. Within the dynamic context: Inertia-aware 3D human modeling with pose sequence. In *ECCV*, 2024. 3
- [5] Wei Cheng, Ruixiang Chen, Siming Fan, Wanqi Yin, Keyu Chen, Zhongang Cai, Jingbo Wang, Yang Gao, Zhengming Yu, Zhengyu Lin, et al. DNA-Rendering: A diverse neural actor repository for high-fidelity human-centric rendering. In *ICCV*, 2023. 2, 4, 5, 6, 8, 15
- [6] Jiankang Deng, Jia Guo, Niannan Xue, and Stefanos Zafeiriou. Arcface: Additive angular margin loss for deep face recognition. In *Proceedings of the IEEE/CVF Conference on Computer Vision and Pattern Recognition (CVPR)*, pages 4690–4699, 2019. 12
- [7] Patrick Esser, Sumith Kulal, Andreas Blattmann, Rahim Entezari, Jonas Müller, Harry Saini, Yam Levi, Dominik Lorenz, Axel Sauer, Frederic Boesel, et al. Scaling rectified flow transformers for high-resolution image synthesis. In *ICML*, 2024. 2, 3, 4
- [8] Artur Grigorev, Michael J Black, and Otmar Hilliges. HOOD: Hierarchical graphs for generalized modelling of clothing dynamics. In *CVPR*, 2023. 3, 12
- [9] Artur Grigorev, Giorgio Becherini, Michael Black, Otmar Hilliges, and Bernhard Thomaszewski. ContourCraft: Learning to resolve intersections in neural multi-garment simulations. *ACM TOG*, 2024. 3, 12, 13
- [10] Chen Guo, Tianjian Jiang, Manuel Kaufmann, Chengwei Zheng, Julien Valentin, Jie Song, and Otmar Hilliges. ReLoo: Reconstructing humans dressed in loose garments from monocular video in the wild. In *ECCV*, 2024. 3
- [11] Michelle Guo, Matt Jen-Yuan Chiang, Igor Santesteban, Nikolaos Sarafianos, Hsiao-yu Chen, Oshri Halimi, Aljaž Božič, Shunsuke Saito, Jiajun Wu, C Karen Liu, et al. PGC: Physics-based gaussian cloth from a single pose. In *CVPR*, 2025. 3
- [12] Marc Habermann, Weipeng Xu, Michael Zollhofer, Gerard Pons-Moll, and Christian Theobalt. DeepCap: Monocular human performance capture using weak supervision. In *CVPR*, 2020. 3
- [13] Sang-Hun Han, Min-Gyu Park, Ju Hong Yoon, Ju-Mi Kang, Young-Jae Park, and Hae-Gon Jeon. High-fidelity 3D human digitization from single 2k resolution images. In *CVPR*, 2023. 4
- [14] Jonathan Ho, Ajay Jain, and Pieter Abbeel. Denoising diffusion probabilistic models. In *NeurIPS*, 2020. 3
- [15] Edward J Hu, Yelong Shen, Phillip Wallis, Zeyuan Allen-Zhu, Yuanzhi Li, Shean Wang, Lu Wang, Weizhu Chen, et al. LoRA: Low-rank adaptation of large language models. In *ICLR*, 2022. 2, 5, 7
- [16] Liangxiao Hu, Hongwen Zhang, Yuxiang Zhang, Boyao Zhou, Boning Liu, Shengping Zhang, and Liqiang Nie. GaussianAvatar: Towards realistic human avatar modeling from a single video via animatable 3D gaussians. *arXiv preprint arXiv:2312.02134*, 2023. 3
- [17] Li Hu, Xin Gao, Peng Zhang, Ke Sun, Bang Zhang, and Liefeng Bo. Animate Anyone: Consistent and controllable image-to-video synthesis for character animation. In *CVPR*, 2024. 3, 4
- [18] Shoukang Hu, Takuya Narihira, Kazumi Fukuda, Ryosuke Sawata, Takashi Shibuya, and Yuki Mitsufuji. HumanGif: Single-view human diffusion with generative prior. *arXiv preprint arXiv:2502.12080*, 2025. 3
- [19] Mustafa İşik, Martin Rünz, Markos Georgopoulos, Taras Khakhulin, Jonathan Starck, Lourdes Agapito, and Matthias Nießner. HumanRF: High-fidelity neural radiance fields for humans in motion. *ACM TOG*, 2023. 2, 4, 5, 6, 8, 15
- [20] Bernhard Kerbl, Georgios Kopanas, Thomas Leimkühler, and George Drettakis. 3D gaussian splatting for real-time radiance field rendering. *ACM TOG*, 2023. 3, 4
- [21] Rawal Khirodkar, Timur Bagautdinov, Julieta Martinez, Su Zhaoen, Austin James, Peter Selednik, Stuart Anderson, and Shunsuke Saito. Sapiens: Foundation for human vision models. In *ECCV*, 2024. 3, 14

- [22] Youngjoong Kwon, Dahun Kim, Duygu Ceylan, and Henry Fuchs. Neural Human Performer: Learning generalizable radiance fields for human performance rendering. In *NeurIPS*, 2021. 2
- [23] Changmin Lee, Jihyun Lee, and Tae-Kyun Kim. MPMA-vatar: Learning 3D gaussian avatars with accurate and robust physics-based dynamics. In *NeurIPS*, 2025. 2, 3
- [24] Zhe Li, Zerong Zheng, Lizhen Wang, and Yebin Liu. Animatable Gaussians: Learning pose-dependent gaussian maps for high-fidelity human avatar modeling. In *CVPR*, 2024. 2
- [25] Philipp Lindenberger, Paul-Edouard Sarlin, and Marc Pollefeys. LightGlue: Local feature matching at light speed. In *ICCV*, 2023. 5
- [26] Ziwei Liu, Ping Luo, Shi Qiu, Xiaogang Wang, and Xiaoou Tang. DeepFashion: Powering robust clothes recognition and retrieval with rich annotations. In *CVPR*, 2016. 4
- [27] Yuxuan Luo, Zhengkun Rong, Lizhen Wang, Longhao Zhang, and Tianshu Hu. DreamActor-M1: Holistic, expressive and robust human image animation with hybrid guidance. In *ICCV*, 2025. 3
- [28] Yifang Men, Yuan Yao, Miaomiao Cui, and Liefeng Bo. MIMO: Controllable character video synthesis with spatial decomposed modeling. In *CVPR*, 2025. 3, 4
- [29] Ben Mildenhall, Pratul P Srinivasan, Matthew Tancik, Jonathan T Barron, Ravi Ramamoorthi, and Ren Ng. NeRF: Representing scenes as neural radiance fields for view synthesis. *Communications of the ACM*, 2021. 3
- [30] Gyeongsik Moon, Takaaki Shiratori, and Shunsuke Saito. Expressive whole-body 3D gaussian avatar. In *ECCV*, 2024. 2, 3, 5, 6
- [31] Arthur Moreau, Jifei Song, Helisa Dharmo, Richard Shaw, Yiren Zhou, and Eduardo Pérez-Pellitero. Human gaussian splatting: Real-time rendering of animatable avatars. In *CVPR*, 2024. 2
- [32] Kiyohiro Nakayama, Jan Ackermann, Timur Levent Kesdogan, Yang Zheng, Maria Korosteleva, Olga Sorkine-Hornung, Leonidas J Guibas, Guandao Yang, and Gordon Wetzstein. Alpparel: A multimodal foundation model for digital garments. In *CVPR*, 2025. 3
- [33] Maxime Oquab, Timothée Darcet, Théo Moutakanni, Huy Vo, Marc Szafraniec, Vasil Khalidov, Pierre Fernandez, Daniel Haziza, Francisco Massa, Alaaeldin El-Nouby, et al. DINOv2: Learning robust visual features without supervision. *arXiv preprint arXiv:2304.07193*, 2023. 3, 14
- [34] Georgios Pavlakos, Vasileios Choutas, Nima Ghorbani, Timo Bolkart, Ahmed AA Osman, Dimitrios Tzionas, and Michael J Black. Expressive body capture: 3D hands, face, and body from a single image. In *CVPR*, 2019. 2
- [35] Sida Peng, Juntong Dong, Qianqian Wang, Shangzhan Zhang, Qing Shuai, Xiaowei Zhou, and Hujun Bao. Animatable neural radiance fields for modeling dynamic human bodies. In *ICCV*, 2021. 2, 3
- [36] Sida Peng, Yuanqing Zhang, Yinghao Xu, Qianqian Wang, Qing Shuai, Hujun Bao, and Xiaowei Zhou. Neural Body: Implicit neural representations with structured latent codes for novel view synthesis of dynamic humans. In *CVPR*, 2021. 2, 3
- [37] Lingteng Qiu, Guanying Chen, Jiapeng Zhou, Mutian Xu, Junle Wang, and Xiaoguang Han. REC-MV: Reconstructing 3D dynamic cloth from monocular videos. In *CVPR*, 2023. 3, 4
- [38] Lingteng Qiu, Xiaodong Gu, Peihao Li, Qi Zuo, Weichao Shen, Junfei Zhang, Kejie Qiu, Weihao Yuan, Guanying Chen, Zilong Dong, and Liefeng Bo. LHM: Large animatable human reconstruction model from a single image in seconds. In *ICCV*, 2025. 1, 2, 3, 5, 6, 7, 8, 12, 13
- [39] Lingteng Qiu, Peihao Li, Qi Zuo, Xiaodong Gu, Yuan Dong, Weihao Yuan, Siyu Zhu, Xiaoguang Han, Guanying Chen, and Zilong Dong. PF-LHM: 3D animatable avatar reconstruction from pose-free articulated human images. *arXiv preprint arXiv:2506.13766*, 2025. 3, 12
- [40] Lingteng Qiu, Shenhao Zhu, Qi Zuo, Xiaodong Gu, Yuan Dong, Junfei Zhang, Chao Xu, Zhe Li, Weihao Yuan, Liefeng Bo, et al. AniGS: Animatable gaussian avatar from a single image with inconsistent gaussian reconstruction. In *CVPR*, 2025. 2, 3, 6, 7
- [41] RenderPeople. [urlhttps://renderpeople.com](https://renderpeople.com), 2025. 4
- [42] Boxiang Rong, Artur Grigorev, Wenbo Wang, Michael J Black, Bernhard Thomaszewski, Christina Tsalicoglou, and Otmar Hilliges. Gaussian Garments: Reconstructing simulation-ready clothing with photorealistic appearance from multi-view video. In *3DV*, 2025. 3
- [43] Ruizhi Shao, Youxin Pang, Zerong Zheng, Jingxiang Sun, and Yebin Liu. 360-degree human video generation with 4D diffusion transformer. *ACM TOG*, 2024. 3
- [44] Geonhee Sim and Gyeongsik Moon. PERSONA: Personalized whole-body 3D avatar with pose-driven deformations from a single image. In *ICCV*, 2025. 2, 3, 4, 5, 6, 8, 12
- [45] Guoxian Song, Hongyi Xu, Xiaochen Zhao, You Xie, Tianpei Gu, Zenan Li, Chenxu Zhang, and Linjie Luo. X-UniMotion: Animating human images with expressive, unified and identity-agnostic motion latents. *arXiv preprint arXiv:2508.09383*, 2025. 3
- [46] Shuyuan Tu, Zhen Xing, Xintong Han, Zhi-Qi Cheng, Qi Dai, Chong Luo, and Zuxuan Wu. StableAnimator: High-quality identity-preserving human image animation. In *CVPR*, 2025. 3, 4
- [47] Ashish Vaswani, Noam Shazeer, Niki Parmar, Jakob Uszkoreit, Llion Jones, Aidan N Gomez, Łukasz Kaiser, and Illia Polosukhin. Attention is all you need. In *NeurIPS*, 2017. 2, 3
- [48] Wenbo Wang, Hsuan-I Ho, Chen Guo, Boxiang Rong, Artur Grigorev, Jie Song, Juan Jose Zarate, and Otmar Hilliges. 4D-DRESS: A 4D dataset of real-world human clothing with semantic annotations. In *CVPR*, 2024. 2, 4, 5, 6, 8
- [49] Zhangyang Xiong, Chenghong Li, Kenkun Liu, Hongjie Liao, Jianqiao Hu, Junyi Zhu, Shuliang Ning, Lingteng Qiu, Chongjie Wang, Shijie Wang, et al. MVHumanNet: A large-scale dataset of multi-view daily dressing human captures. In *CVPR*, 2024. 4, 5
- [50] Wangze Xu, Yifan Zhan, Zhihang Zhong, and Xiao Sun. Sequential gaussian avatars with hierarchical spatio-temporal context. In *ICCV*, 2025. 2, 3, 6

- [51] Zhongcong Xu, Jianfeng Zhang, Jun Hao Liew, Hanshu Yan, Jia-Wei Liu, Chenxu Zhang, Jiashi Feng, and Mike Zheng Shou. MagicAnimate: Temporally consistent human image animation using diffusion model. In *CVPR*, 2024. 3, 4
- [52] Zhendong Yang, Ailing Zeng, Chun Yuan, and Yu Li. Effective whole-body pose estimation with two-stages distillation. In *ICCVW*, 2023. 6
- [53] Wanqi Yin, Zhongang Cai, Ruisi Wang, Ailing Zeng, Chen Wei, Qingping Sun, Haiyi Mei, Yanjun Wang, Hui En Pang, Mingyuan Zhang, et al. SMPLest-X: Ultimate scaling for expressive human pose and shape estimation. *arXiv preprint arXiv:2501.09782*, 2025. 6
- [54] Tao Yu, Zerong Zheng, Kaiwen Guo, Pengpeng Liu, Qionghai Dai, and Yebin Liu. Function4D: Real-time human volumetric capture from very sparse consumer rgbd sensors. In *CVPR*, 2021. 4
- [55] Youyi Zhan, Tianjia Shao, Yin Yang, and Kun Zhou. Real-time high-fidelity gaussian human avatars with position-based interpolation of spatially distributed mlps. In *CVPR*, 2025. 3
- [56] Richard Zhang, Phillip Isola, Alexei A Efros, Eli Shechtman, and Oliver Wang. The unreasonable effectiveness of deep features as a perceptual metric. In *CVPR*, 2018. 5, 6
- [57] Yuang Zhang, Jiayi Gu, Li-Wen Wang, Han Wang, Junqi Cheng, Yuefeng Zhu, and Fangyuan Zou. MimicMotion: High-quality human motion video generation with confidence-aware pose guidance. In *ICML*, 2025. 3, 5, 13
- [58] Zerong Zheng, Xiaochen Zhao, Hongwen Zhang, Boning Liu, and Yebin Liu. AvatarRex: Real-time expressive full-body avatars. *ACM TOG*, 2023. 2, 3
- [59] Yi Zhou, Connelly Barnes, Jingwan Lu, Jimei Yang, and Hao Li. On the continuity of rotation representations in neural networks. In *CVPR*, 2019. 4, 14
- [60] Shenhao Zhu, Junming Leo Chen, Zuozhuo Dai, Zilong Dong, Yinghui Xu, Xun Cao, Yao Yao, Hao Zhu, and Siyu Zhu. Champ: Controllable and consistent human image animation with 3D parametric guidance. In *ECCV*, 2024. 3
- [61] Yiyu Zhuang, Jiayi Lv, Hao Wen, Qing Shuai, Ailing Zeng, Hao Zhu, Shifeng Chen, Yujie Yang, Xun Cao, and Wei Liu. IDOL: Instant photorealistic 3D human creation from a single image. In *CVPR*, 2025. 2, 3, 4, 5, 6, 7, 8, 12, 13

## Supplementary Material for

# “Zero-Shot Reconstruction of Animatable 3D Avatars with Cloth Dynamics from a Single Image”

Joohyun Kwon    Geonhee Sim    Gyeongsik Moon  
Korea University

{juheanqueen, kh6362, mks0601}@korea.ac.kr

<https://juhyeon-kwon.github.io/DynaAvatar.github.io/>

In this supplementary material, we provide more experiments, discussions, and other details that could not be included in the main text due to the lack of pages. The contents are summarized below:

- Sec. S1: Comparisons to related works
- Sec. S2: Dataset reannotation comparisons
- Sec. S3: Ablation studies
- Sec. S4: Architecture details
- Sec. S5: Implementation details

## S1. Comparisons to related works

We compare DynaAvatar with state-of-the-art methods, physics-based approaches, and diffusion-based approaches to show its advantages. Please refer to the accompanying supplementary video for the full animation results.

### S1.1. Comparison to state-of-the-art methods

#### S1.1.1. Qualitative comparisons

Fig. S1 shows comparisons of our DynaAvatar and previous state-of-the-art methods [38, 44, 61] from in-the-wild input image. Our method successfully reconstructs and animates avatars with high-fidelity cloth dynamics. For instance, when the subject raises their arms, the upper garment naturally lifts upward, exhibiting physically plausible motion-dependent dynamics.

In contrast, baseline methods generate animations without incorporating motion-dependent dynamics. Consequently, the resulting animations often lack realism, as the garments remain static regardless of the body’s movement. Our method effectively overcomes this limitation by leveraging the Dynamic Transformer, resulting in superior visual realism.

Note that PF-LHM [39] is excluded due to code unavailability. Nevertheless, as it takes only the pose cues without motion information (*i.e.*, a sequence of poses), similar to PERSONA [44], it is expected to lack the capability to represent motion-dependent dynamics, thereby underperforming compared to our motion-aware approach.

#### S1.1.2. Quantitative comparisons

**Face consistency.** Table. S1 on DNA-Rendering shows that DynaAvatar achieves superior image consistency, as shown by the higher face consistency (FC) compared to

Table S1. Comparison of face consistency (FC) on DNA-Rendering.

Methods	FC $\uparrow$
IDOL [60]	0.625
LHM [37]	0.697
<b>DynaAvatar (Ours)</b>	<b>0.712</b>

Table S2. Comparison of computational costs.

Methods	Zero-shot	Cloth dynamics	Time	# of params.
PERSONA [43]	$\times$	$\checkmark$	3.11h	4M
LHM-500M [37]	$\checkmark$	$\times$	1.08s	356M
LHM-1B [37]	$\checkmark$	$\times$	3.00s	1.1B
<b>DynaAvatar (Ours)</b>	$\checkmark$	$\checkmark$	1.82s	719M

baseline methods. FC is measured via cosine similarity in the ArcFace [6] embedding space.

**Inference Latency.** As shown in Table. S2, DynaAvatar ensures fast inference via its zero-shot architecture, avoiding the lengthy per-subject optimization of PERSONA. While our Dynamic Transformer adds moderate overhead compared to LHM-500M, it remains more efficient than LHM-1B in both time and parameters. This cost is essential for capturing dynamic deformations, offering a superior trade-off for motion-dependent cloth dynamics that LHM lacks. All metrics are measured on a RTX pro 6000 GPU.

### S1.2. Comparison to physics-based approaches

Fig. S2 compares the physics-based method [8, 9] with DynaAvatar, highlighting the instability of the former under in-the-wild scenarios. Note that we used a garment template of a similar type to the input image for the physics-based simulation. As shown in the Fig. S2 left, applying physics simulation to in-the-wild sequences often leads to catastrophic failures where the cloth unrealistically flies away or drifts. This instability stems from the imperfect in-the-wild pose estimation. Specifically, pose errors frequently cause the body mesh to penetrate the garment mesh, creating invalid collision constraints. These interpenetrations trigger erroneous inputs in the simulation, causing garment to become unstable. Moreover, these methods primarily focus on geo-

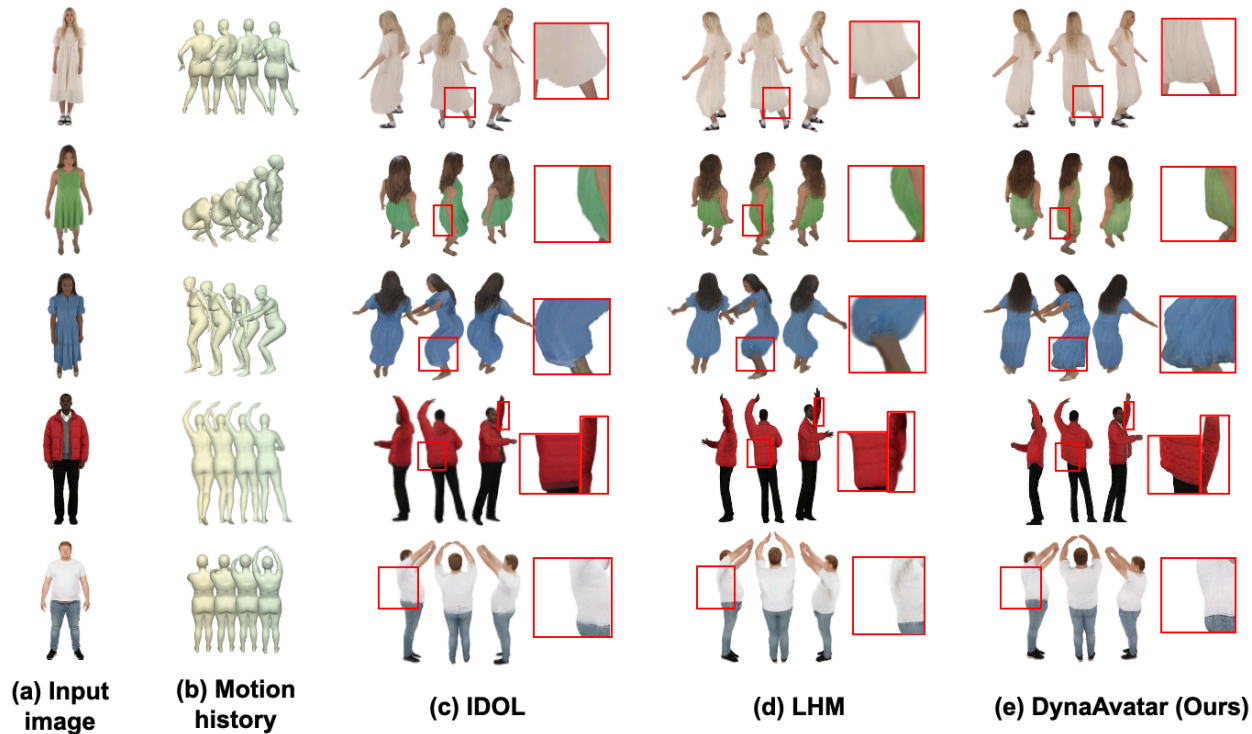


Figure S1. Comparison between DynaAvatar and previous single-image-based state-of-the-art methods [38, 61] on in-the-wild images.

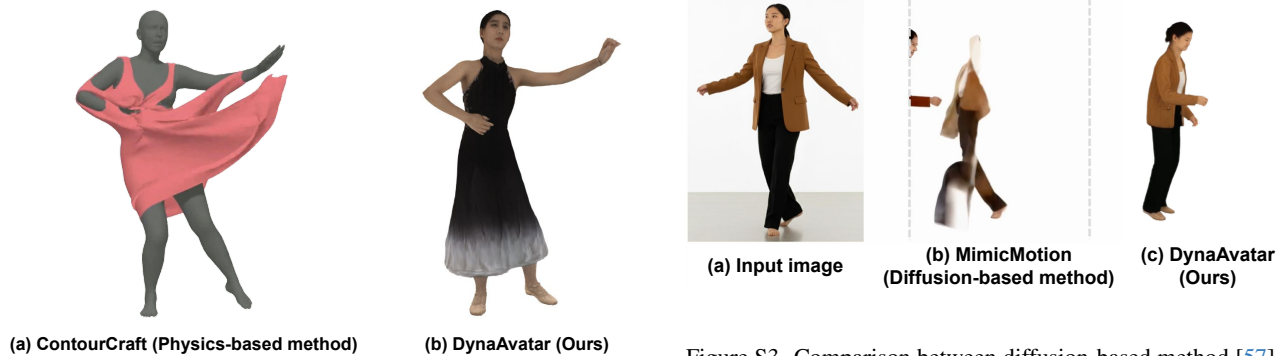


Figure S2. Comparison between physics-based method [9] and DynaAvatar.

metric garment deformation, often lacking the capability to model photorealistic, full-body appearance.

In contrast, DynaAvatar robustly synthesizes both motion-dependent cloth dynamics and high-fidelity appearance, even when driven by in-the-wild motion sequences. These results validate DynaAvatar as a robust and practical method for animating avatars from single images.

Figure S3. Comparison between diffusion-based method [57] and DynaAvatar.

### S1.3. Comparison to diffusion-based approaches

Fig. S3 compares the state-of-the-art diffusion-based method [57] with DynaAvatar, highlighting the limitations of diffusion models. These models fundamentally require pixel-level alignment between the reference image and the target pose. When this constraint is violated due to large global motion, the generated results suffer from severe degradation, exhibiting noticeable artifacts and hallucinations.

Moreover, since diffusion-based methods predominantly center the target pose along the  $y$ -axis within a fixed output

Table S3. Effectiveness of our dataset reannotations on 4D-Dress.

Settings	PSNR $\uparrow$	SSIM $\uparrow$	LPIPS $\downarrow$
(1)	20.72	0.952	0.085
(2)	20.91	0.953	0.084
<b>(3) (Ours)</b>	<b>23.74</b>	<b>0.960</b>	<b>0.064</b>

resolution, body parts such as arms are frequently cropped. Furthermore, significant movement along the  $x$ -axis often causes the subject to move out of frame, cutting off parts of the animation.

In contrast, DynaAvatar is free from these alignment constraints and robustly handles large global motions. This capability stems from our Dynamic Transformer, which effectively incorporates motion features via attention mechanisms without relying on explicit spatial alignment.

## S2. Dataset Reannotation comparisons

Fig. S4 provides additional comparisons between (b) the original SMPL-X fittings and (c) our reannotated results. Our reannotations produce more accurate and visually plausible poses, whereas the original annotations often contain noisy predictions and noticeable temporal jitter. Such instability in the original annotations hinders learning a reliable and practical relationship between human motion and cloth deformation. In contrast, our reannotated sequences exhibit significantly improved temporal consistency and pose accuracy. As a result, our reannotated datasets are directly usable for training motion-dependent deformation models.

## S3. Ablation studies

We provide additional ablation study results to validate our design choices.

### S3.1. Dataset reannotations

Table S3 on 4D-Dress shows the value of our reannotations by fixing the architecture while varying training annotations. We compare three settings: (1) the original annotations, (2) reannotation of the originally available frames, and (3) our fully reannotated dataset (Sec. 4). Results show that our reannotations (3) yield far superior results compared to the original annotations (1), which suffers from 80% missing frames. Fig. 4 and Sec. S2 additionally show the value of our reannotations.

## S4. Architecture details

Fig. 2 and Sec. 3.1 of the main manuscript show architecture of the proposed DynaAvatar. We provide detailed descriptions of each component.

### S4.1. Static Transformer

The Static Transformer takes two distinct image tokens: body tokens and head tokens, extracted via Sapiens [21] and DINOv2 [33], respectively. It consists of several layers, each of which is composed of a Body Transformer block and a Head Transformer block. The Body Transformer block utilizes the body tokens as key and value to update the input query tokens, whereas the Head Transformer block utilizes the head tokens. Additionally, we compute the global average of the body tokens and inject this feature into the Static Transformer through adaptive Layer Normalization (AdaLN) [?].

### S4.2. Motion encoder

The Motion encoder is designed as a simple MLP that takes the motion history as input and outputs motion tokens. We construct a motion history representation from the pose sequence, which consists of  $K = 22$  body joints. For a pose sequence with  $T$  frames, we concatenate the 3D joint linear velocities, 6D rotation-parameterized [59] pose, pose velocity, and pose acceleration, resulting in a 21-dimensional motion vector per joint. This motion history is flattened to form a tensor of shape  $\mathbb{R}^{T \times (K \cdot 21)}$ , which is subsequently mapped to  $T$  motion tokens via the motion encoder.

### S4.3. Dynamic Transformer

The Dynamic Transformer utilizes the encoded motion tokens to update the query features output by the Static Transformer. Unlike the Static Transformer layer, which comprises two distinct blocks, Dynamic Transformer layer is implemented as a single block where motion tokens act as keys and values. Furthermore, the last element of the motion tokens is injected via AdaLN to explicitly provide the target pose context.

## S5. Implementation details

We observed that constructing a batch with a single subject across multiple timeframes and views yields better convergence than stacking multiple subjects. Accordingly, for the training of DynaAvatar, we configure the batch with  $F = 4$  temporal frames and  $V = 4$  views per subject, resulting in a batch size of 16. Our model is trained using the AdamW optimizer with an initial learning rate of  $4 \times 10^{-4}$  and gradient clipping set to 0.1. We apply LoRA to all linear layers in the Static Transformer with a rank  $r = 32$ , scaling alpha  $\alpha = 64$ , and a dropout rate of 0.1. The training is conducted on 8 NVIDIA RTX Pro 6000 GPUs for a total of 40K iterations, taking approximately 90 hours. The DynaFlow loss is activated after 20K iterations to ensure that a coarse geometry is established.

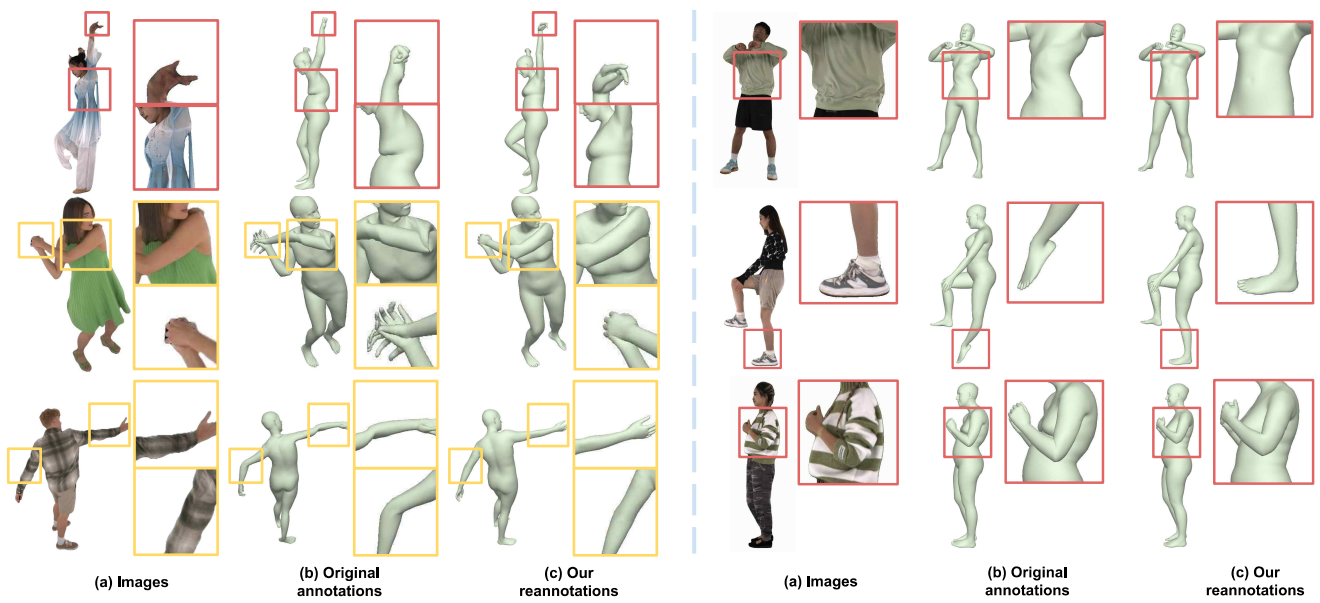


Figure S4. Comparison between (b) the original annotations and (c) our reannotations. The bounding box colors indicate the source datasets: **Red** denotes DNA-Rendering [5], and **Yellow** denotes Actors-HQ [19].